Journal of Statistical Physics, Vol. 82, Nos. 3/4, 1996

A Monte Carlo Algorithm for Lattice Ribbons

E. Orlandini,[1] E. J. Janse van Rensburg,[2] and S. G. Whittington[3]

Received February 20, 1995; final June 19, 1995

A lattice ribbon is a connected sequence of plaquettes subject to certain self-avoidance conditions. The ribbon can be closed to form an object which is topologically either a cylinder or a Möbius band, depending on whether its surface is orientable or nonorientable. We describe a grand canonical Monte Carlo algorithm for generating a sample of these ribbons, prove that the associated Markov chain is ergodic, and present and discuss numerical results about the dimensions and entanglement complexity of the ribbons.

KEY WORDS: Ribbon; lattice models; Monte Carlo algorithm; knotting and linking; entanglements.

1. INTRODUCTION

Self-avoiding walks have been studied for many years as a model of long-chain polymers in dilute solution in a good solvent.[1] This model retains the two essential features of connectivity and excluded volume, and has become accepted as the simplest model which adequately describes this physical system. It has been modified in many ways. By converting the walk to a polygon one can investigate topological features such as knotting,[2] and by adding a short-range attractive potential one can model the collapse transition from a coil to a ball at the theta temperature.[3]

Some polymer molecules appear in a duplex form in which one strand winds around the other. The classic example is DNA,[4,5] but the phenomenon also occurs in polysaccharides such as the carageenans.[6] If the polymer is closed to form two intertwined rings, the rings can be linked as

[1] Department of Theoretical Physics, Oxford, England, OX1 3NP.
[2] Department of Mathematics and Statistics, York University, North York, Ontario, Canada, M3J 1P3.
[3] Department of Chemistry, University of Toronto, Toronto, Ontario, Canada, M5S 1A1.

0022-4715/96/0200-1159$09.50/0

well as knotted. This situation has been modeled as a ribbon, in which the two polymers are modeled as the two boundary curves of the ribbon.[4]

In order to understand the asymptotic behavior (as the polymers become very long), we introduced[7] a lattice ribbon model of such double-stranded molecules, where the ribbon is made up of a sequence of plaquettes (unit squares in the cubic lattice). The model is designed to retain the simplicity of the self-avoiding walk, while having the richness of the ribbon model. The model has the advantage that some of its properties can be established rigorously (using techniques borrowed from the theory of self-avoiding walks) and its discrete nature makes it particularly suitable for study by Monte Carlo techniques. Linking, twisting, and writhing are natural properties of the model, and it can be enhanced by adding fugacity terms to increase the extent of twisting or writhing.

This paper is concerned with the basic Monte Carlo algorithm which we have developed and its application to the simplest situation: a closed ribbon with no added fugacities for twist or writhe. In Section 2 we define the model and introduce a Markov chain Monte Carlo algorithm. Section 3 is devoted to the reversibility and ergodicity properties of the Markov chain: In particular, we derive an invariant limit distribution by proving reversibility and irreducibility, conditional on the inclusion of a certain set of elementary transitions in the Markov chain. We also describe an algorithm for simulating closed ribbons whose axis is a fixed knot type. The implementation of the algorithm is described in Section 4, where particular attention is paid to data structures. Numerical results are presented in Section 5. We compute autocorrelation times to study the correlations of the Markov chain, and compute the growth constant and entropic and metric exponents for ribbons. The metric exponent ν is close to that of self-avoiding walks. We next turn our attention to the entanglement complexity of ribbons and compute the linking between boundary components and the writhe of the ribbon. We also consider the knot type of the boundary curve in nonorientable ribbons. The paper concludes in Section 6 with a few final observations and remarks.

2. A MONTE CARLO ALGORITHM FOR LATTICE RIBBONS

A unit square with vertices with integer coordinates is a *plaquette* in the cubic lattice Z^3. Two plaquettes are adjacent if they share exactly one edge. A *closed* ribbon is an ordered sequence of plaquettes $\{\sigma_0, \sigma_1, ..., \sigma_{n-1}\}$ such that:

1. Two plaquettes i and j are incident on a common edge if and only if $|i-j| = 1$ or $n-1$.

2. If two plaquettes are nonadjacent, then they can share a vertex only if they are both adjacent to the same plaquette.
3. No more than three plaquettes can be incident on the same vertex.

If and edge e is the intersection of adjacent plaquettes ($e=\sigma_i \cup \sigma_{(i+1) \bmod n}$, for some i), then we call e a *ribbon edge*, otherwise it is a *boundary edge*. Observe that ribbon edges are incident on exactly two plaquettes, while boundary edges are incident on only one plaquette.

The intersection $\sigma_{(i-1) \bmod n} \cap \sigma_i \cap \sigma_{(i+1) \bmod n}$ is either empty or consists of exactly one vertex incident on the three plaquettes, for any i. If it is empty, then σ_i is an *ordinary* plaquette, otherwise it is a *corner* plaquette. These cases are illustrated in Fig. 1. An ordinary plaquette has opposite edges on the boundary of the ribbon, while a corner plaquette has two adjacent edges on the boundary of the ribbon, and one vertex incident on both its nearest neighbors in the ribbon (indicated by • in Fig. 1b).

A ribbon is *open* if its first and last plaquettes are not adjacent and have empty intersection. The number of ribbon edges incident on a plaquette is its *degree*. In a closed ribbon every plaquette has degree 2, but in an open ribbon the first and last plaquettes have degree 1, while all other plaquettes have degree 2. We write w_n for the number of open ribbons with n plaquettes, where two ribbons are considered distinct if they can not be superimposed by translation. Closed ribbons can be orientable (i.e., having two boundary curves) or nonorientable (having only one boundary curve). We write r_n for the number of closed ribbons with n plaquettes, and respectively r_n^o and r_n^u for the numbers of closed ribbons with n plaquettes which are orientable and nonorientable: clearly $r_n = r_n^o + r_n^u$.

The number of distinct open ribbons grows exponentially fast with n, the number of plaquettes. The *growth constant* ρ measures the rate of exponential growth, and it is defined by $\log \rho = \lim_{n \to \infty} n^{-1} \log w_n$ (this limit exists by concatenation arguments). Moreover, upper and lower bounds may be derived on ρ: $4 \leqslant \rho \leqslant 9$. Similar techniques may be used to prove the existence of a growth constant for closed ribbons, and for orientable and nonorientable ribbons as well. In all three cases it is equal to ρ.[7]

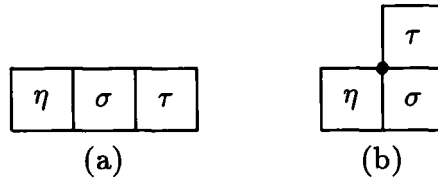

Fig. 1. (a) An ordinary plaquette and (b) a corner plaquette.

If an open (closed) ribbon is collapsed onto its centerline, then we find a self-avoiding walk (polygon) in a decorated cubic lattice. Hence, a ribbon should be in the same universality class as walks, and critical exponents for ribbons should be equal to those for walks. If R_n^2 is the mean square radius of gyration of an open or a closed ribbon with n plaquettes, then it is believed that

$$\begin{aligned} R_2 &\sim n^{2\nu} \\ w_n &\sim n^{\gamma-1}\rho^n \\ r_n &\sim n^{\alpha-3}\rho^n \end{aligned} \tag{2.1}$$

where we expect $\nu \sim 0.588$ for the metric exponent, and $\gamma \sim 1.1615$ and $\alpha \sim 0.25$[8] for the entropic exponents. On the other hand, ribbons have more local structure than walks: in particular, the two boundary curves of a closed orientable ribbon may be linked. A theorem in differential geometry[9–11] decomposes the linking number Lk of these boundary curves into the twist Tw of one boundary about the centerline of the ribbon and writhe Wr of the centerline as

$$Lk = Tw + Wr \tag{2.2}$$

The knot type of the centerline of the ribbon as well as Tw, Wr, and Lk are measures of entanglement of the ribbon. These data are known to be important in determining the physical complexity of DNA.[5, 12]

A numerical method to simulate closed ribbons would be particularly useful in understanding the decomposition in Eq. (2.2). In Section 2.1 we describe a Monte Carlo algorithm for realizing a Markov chain defined on the set of closed ribbons at a fixed plaquette fugacity K in the *grand canonical ensemble.* The statistics of the realized ribbons is described by a generating function of the general form

$$G_\kappa(K) = \sum_{n=1}^{\infty} r_n K^n n^\kappa \tag{2.3}$$

where κ is an integer which will be determined by the particular implementation of the algorithm. κ has no physical meaning, but we can tune the distribution from which we sample by varying K and κ, allowing us to focus the sampling on ribbons of different lengths (see Sections 4.1 and 5.3 for details). The fugacity is related to a chemical potential μ of the plaquettes by $K = e^\mu$. The algorithm will rely on two kinds of elementary transitions between states: the first is a local move, which changes a small number of

neighboring plaquettes locally, while the second kind is a global move, reminiscent of "pivot" moves employed in the simulation of polygons in the cubic lattice.[13]

2.1. Local Elementary Transitions

The local part of the algorithm, which is a *grand canonical* implementation (since it involves changing the number of plaquettes in the ribbon), uses local elementary transitions of three different types. These are dubbed *corner*, *ordinary*, and *double* moves. We describe these in turn:

Corner Moves. Let $\sigma = \sigma_i$ be a corner plaquette and let $\eta = \sigma_{(i-1) \bmod n}$ and $\tau = \sigma_{(i+1) \bmod n}$ be its neighboring plaquettes. Let $\bullet = \eta \cap \sigma \cap \tau$. There are four edges incident on $\bullet$: the two ribbon edges incident on σ and η, and on σ and τ respectively, and two boundary edges, one incident on η and the other incident on τ.

Remove σ from the ribbon and select with uniform probability, by using, for example, rejection techniques, two of the four edges incident on $\bullet$ perpendicular to each other, and such that one is incident on η and the other is incident of τ. These selected edges will be the new ribbon edges; a plaquette is added back between them as illustrated in Fig. 2, and the resulting conformation is accepted as a newly proposed ribbon if it is a ribbon. If the resulting conformation is not a ribbon, then it is rejected, and the old ribbon is repeated in the realization of the Markov chain.

Ordinary Moves. Ordinary moves are executed on ordinary plaquettes in the ribbon, and they may involve length changes through the addition or substraction of plaquettes from the ribbon. There are two flavors of these moves: a *parallel shift* and a 90° *rotation*. Let σ be an ordinary plaquette, with neighbors η and τ and second nearest neighbors η' and τ' (η' on the side of η and τ' on the side of τ) in the ribbon.

A *parallel shift* is attempted on σ by translating σ parallel to itself a unit distance in the lattice through one of its boundary edges. Label the

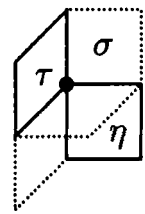

Fig. 2. The corner move can be carried out by removing σ and by putting it back between η and τ.

translated plaquette σ'. There are three cases. Case (1): Suppose that σ' is disjoint with η' and τ'. Then the ribbon is disconnected. It can be reconnected by adding plaquettes between the old ribbon edges of σ' and a boundary edge on each of η and τ, as illustrated in Fig. 3, case (1). Then η and τ become new second nearest neighbor plaquettes to σ', and the number of plaquettes in the new conformation has increased by two. If the old ribbon edges on σ' are incident on one boundary edge from each of η' and τ', then we have case (2), which is the inverse of case (1). These boundary edges now become ribbon edges, and η and τ are removed from the ribbon. The transition is illustrated in Fig. 3 by reading case (1) from right to left. The number of plaquettes in the ribbon is reduced by two. Case (3) in the parallel shift move occurs when σ' is incident on one boundary edge of one of its second nearest neighbors, say τ', and disjoint with the other (η). Remove τ and add a plaquette incident on the old ribbon edge of σ' and with a boundary edge of η. This move is length preserving and illustrated in Fig. 3. It is its own inverse move.

A 90° *rotation* is attempted by selecting an ordinary plaquette and rotating it randomly (either in a positive or in a negative sense) through 90° about one of its boundary edges. The possible resulting changes in conformation depend on the local structure of the ribbon, and these are illustrated in Fig. 4.

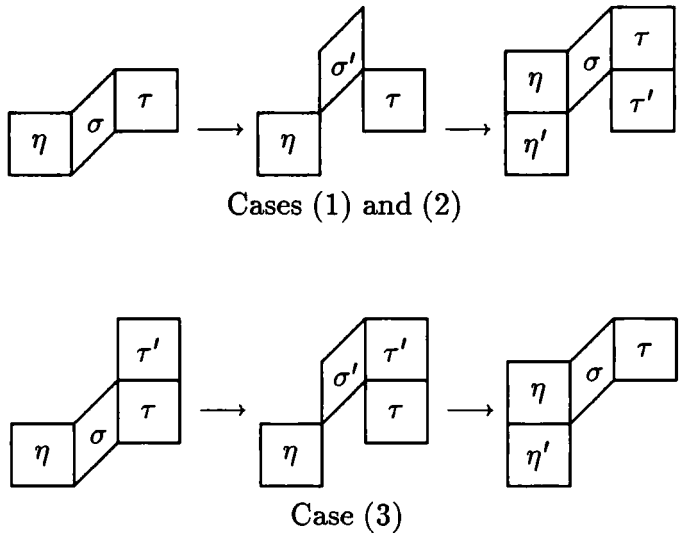

Fig. 3. The possible outcomes of the parallel shift.

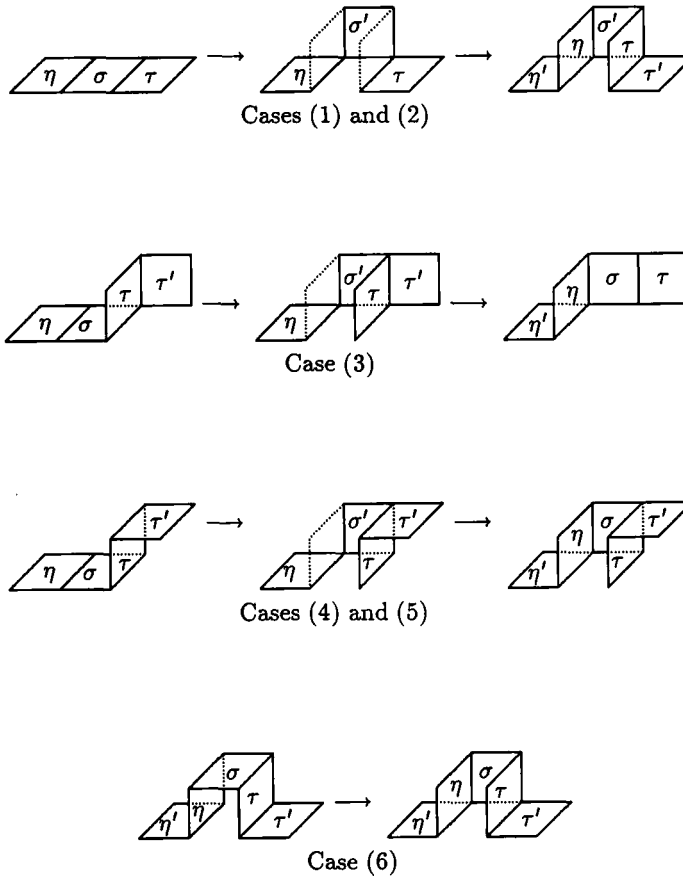

Fig. 4. Possible outcomes in the 90° rotation.

The cases in Fig. 4 can be classified by determining the positions of the two ribbon edges of σ after the rotation: Each ribbon edge $e = \sigma \cap \eta$ (or $e' = \sigma \cap \tau$) may be rotated to be (a) disjoint with η (τ), or (b) onto a boundary edge of η (τ), or (c) onto the ribbon edge $\eta \cap \eta'$ ($\tau \cap \tau'$). Since each of these may occur at either ribbon edge of σ, there is a total of nine possible outcomes, but some of these are the equivalent under exchange of η and τ. If (a) above occurs at e and e', then we refer to that outcome as case (aa). Similarly, we also find cases (ab), (ac), (bb), (bc), and (cc). These cases are illustrated in Fig. 4, with case (1) equivalent to (aa), (2) to (cc), (3) to (ac), (4) to (ab), (5) to (bc), and (6) to (bb). In some of these cases, plaquettes must be added or deleted to maintain the integrity of the ribbon.

If e (or e') is rotated disjoint with η (τ), then a plaquette is added incident on e and the old ribbon edge of η (τ) [which occurs whenever case (a) above is the case]. In case (b), no plaquette is added, but observe that a boundary edge becomes a ribbon edge, and vice versa. In case (c), η (τ) must be removed, since there are now three plaquettes incident on the edge $\eta' \cap \eta$ ($\tau \cap \tau'$). Taken together, the length changes of the ribbon in the six distinct cases are $+2$ in case (1), $+1$ in case (4), 0 in cases (3) and (6), -1 in case (5), and -2 in case (2). Incidently, note that every case is reversible; cases (1) and (2) and cases (4) and (5) are inverses of each other, while cases (3) and (6) are their own inverses.

A *double move* can be performed on adjacent plaquettes with the same orientation (parallel normal vectors). Adjacent pairs of plaquettes must be selected with uniform probability to attempt the move (this can be achieved, for example, by selecting a ribbon edge with uniform probability). If the adjacent plaquettes do not have the same orientation, then the move is rejected. Let σ_1 and σ_2 be two adjacent plaquettes with the same orientation. Suppose that η and η' are the neighbor and second neighbor of σ_1 in the ribbon, and τ and τ' are the neighbor and second neighbor of σ_2. Moreover, let $e_1 = \sigma_1 \cap \tau$ be the ribbon edges between the σ_i and their neighbors ($i = 1, 2$). The double move is attempted by translating $\sigma_1 \cup \sigma_2$ one lattice spacing in the direction, or against the direction, of their normal vectors. The fate of the edges e_1 and e_2 determines the outcome of the attempt, exactly by the same rules applied to the 90° rotation above: Case (a) occurs when e_1 is moved to a position disjoint with η, case (b) when e_1 is moved onto a boundary edge of η, or (c) onto the ribbon edge $\eta \cap \eta'$. The situation with e_2 gives the same possible outcomes, with η replaced by τ. (Observe that there is no difference between the cases with σ_1 and σ_2 corner or ordinary plaquettes; the three cases above are independent of this.)

The same arguments used for 90° rotations produce six distinct possible outcomes illustrated in Fig. 5. In the same notation, case (1) corresponding to case (aa), (2) to (cc), (3) to (ac), (4) to (ab), (5) to (bc), and (6) to (bb). If e_1 is moved to a position disjoint with η [case (a) above], then an extra plaquette must be added to reconnect the ribbon; this is done between the old and new positions of e_1, as illustrated in Fig. 5, case (1). If case (b) is presented, then no plaquette is added, but observe that a boundary edge becomes a ribbon edge and vice versa. In case (c) there are three plaquettes incident on the edge $\eta \cap \eta'$, and η must be deleted to maintain the integrity of the ribbon. Equivalent arguments and constructions are valid if e_2 is considered instead. Consequently, the six distinct cases in Fig. 5 may increase the length of the ribbon by 2 [case (1)] or by 1 [case (4)] or leave it unchanged [cases (3) and (6)],

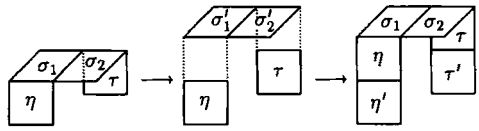

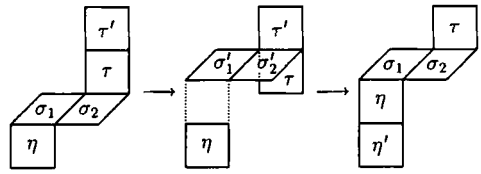

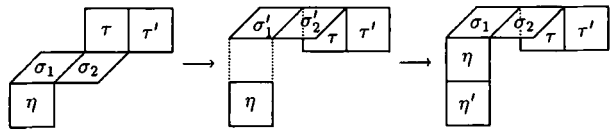

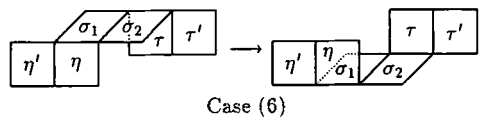

Fig. 5. The possible outcomes of a double move.

or decrease the length by 1 [case (5)] or by 2 [case (2)]. Observe that every case is reversible; cases (1) and (2) and cases (4) and (5) are inverses, and cases (3) and (6) are their own inverses.

3. REVERSIBILITY AND REDUCIBILITY

It is apparent that the elementary moves described in Section 2 will not be able to untie a ribbon with a knotted axis (the axis of the ribbon is found by connecting the midpoints of successive ribbon edges), so the Markov chain is reducible. It will be made irreducible by the addition of a global move. In order to understand what we need to do to obtain an irreducible algorithm, it is necessary to understand the reducibility properties of the current algorithm. A second issue, which we discuss first, is

reversibility, and the nature of the invariant limit distribution within an ergodicity class. We focus on a proof of reversibility for the case $\kappa = 1$ in Eq. (2.3); the implementation of the algorithm for other values of κ is discussed in Section 4.1.

3.1. Reversibility

Implementation of the algorithm is "Metropolis style"[14]; the relative weight as a function of the fugacity of a proposed conformation is computed and accepted with the Metropolis rule. Let R_1 be the current ribbon with length $|R_1|$. The relative weight of R_1 is $K^{|R_1|}$. If the newly proposed ribbon has length $|R_2|$, then we accept it with probability $K^{|R_2|-|R_1|}$ if $|R_2| > |R_1|$ and with probability 1 otherwise, as the next state in the realization of the Markov chain. The implementation and reversibility equations are as follows:

1. With probability q, attempt a double move by selecting a ribbon edge in R_1 at random. If the two plaquettes incident on this ribbon edge have the same orientation, then the move is attempted, otherwise the attempt is rejected and R_1 is the next state in the Markov chain. If an intersection occurs, or if implementing the move results in a conformation which is not a ribbon, then the attempt is rejected, and R_1 is the next state in the Markov chain. Let R_2 be the newly proposed ribbon. If $|R_1| \geqslant |R_2|$, accept R_2 as the new state, otherwise accept R_2 as the new state with probability $K^{|R_2|-|R_1|}$. Therefore

$$\text{Prob}\{R_1 \to R_2\} = \frac{q}{2|R_1|} \begin{cases} 1, & \text{if } |R_1| \geqslant |R_2| \\ K^{|R_2|-|R_1|}, & \text{otherwise} \end{cases} \tag{3.1}$$

Since every double move has an inverse by design, detailed balance follows by exchanging R_1 and R_2 in Eq. (3.1):

$$|R_1| \text{ Prob}\{R_1 \to R_2\} K^{|R_1|} = |R_2| \text{ Prob}\{R_2 \to R_1\} K^{|R_2|} \tag{3.2}$$

2. Otherwise, with probability $(1-q)$, attempt one of the other available moves. Select a plaquette in R_1 with uniform probability. If the plaquette is a corner plaquette, then a corner move is attempted, described in 2(a) below, otherwise, a parallel shift or a 90° rotation is attempted, described in 2(b).

2(a). Let m be the total number of possible corner plaquettes which can be put between the neighbors of the selected plaquette ($m = 3$ in Fig. 2).

Move the corner plaquettes and reject the move if an intersection occurs. Otherwise, ribbon R_2 with $|R_1| = |R_2|$ is the outcome, and

$$\text{Prob}\{R_1 \to R_2\} = (1-q)/(m\,|R_1|) \tag{3.3}$$

Interchanging R_1 and R_2 gives Eq. (3.2), since $|R_1| = |R_2|$

2(b). With probability p attempt a parallel shift move, and with probability $(1-p)$ attempt a 90° rotation. Since the selected plaquette may be shifted in two possible directions, a ribbon R_2 is obtained from R_1 with probability

$$\text{Prob}\{R_1 \to R_2\} = \frac{(1-q)\,p}{2\,|R_1|} \begin{cases} 1 & \text{if } |R_1| \geqslant |R_2| \\ K^{|R_2|-|R_1|} & \text{otherwise} \end{cases} \tag{3.4}$$

where the possible length changes were considered as with the double move. If an overlap occurs in the proposed R_2, then the attempt is rejected. On the other hand, if a 90° rotation is attempted, then the selected plaquette may be rotated about each boundary edge in two possible ways, for a total of four possible rotations. Hence R_2 is obtained with probability

$$\text{Prob}\{R_1 \to R_2\} = \frac{(1-q)(1-p)}{4\,|R_1|} \begin{cases} 1 & \text{if } |R_1| \geqslant |R_2| \\ K^{|R_2|-|R_1|} & \text{otherwise} \end{cases} \tag{3.5}$$

and if an intersection occurs, then the attempt is rejected. If the moves and states are reversed in Eq. (3.4) and (3.5), then Eq. (3.2) is recovered, since every possible transition was designed to have an inverse move.

In each of these cases, we recover Eq. (3.2), and so it describes the reversibility properties of the algorithm. By summing Eq. (3.2) over R_2 the invariant limit distribution is nr'_nK^n, where r'_n is the number of ribbons on n plaquettes, within an unspecified ergodicity class of the algorithm. In the next section we specify the ergodicity classes.

3.2. Reducibility

Let R_0 be a ribbon and implement the Monte Carlo algorithm as set out in Section 3.1. If we initialize the algorithm with R_0, then a Markov chain with states $\{R_0, R_1, ..., R_i, ...\}$ is realized. Let $\text{Prob}^n(R_i \to R_j)$ be the probability that R_j will be realized in the chain, after exactly n iterations, if the algorithm is initialized at R_i. Let $\mathscr{R}$ be the set of all ribbons, and define

$$\mathscr{E}(R_0) = \{R \in \mathscr{R} \mid \text{Prob}^n(R_0 \to R) > 0 \text{ for } n < \infty\} \tag{3.6}$$

In other words, $\mathscr{E}(R_0)$ is the subset of all ribbons which may be realized with positive probability in a Markov chain initialized at R_0. The elements of $\mathscr{E}(R_0)$ are the consequents of R_0. If $\mathscr{E}(R_0) = \mathscr{R}$, then the algorithm realizes an irreducible Markov chain; one also says that the chain is *ergodic* (it is aperiodic). Otherwise the chain is reducible, and it remains to characterize the "ergodicity classes" $\mathscr{E}(R_0)$.

If the barycenters of adjacent plaquettes are joined by edges, then we find the *center polygon* of the ribbon. The knot type of the ribbon is defined as that of its center polygon. Local transitions as proposed in Section 2.1 induce local deformations of the center polygon; the center polygon is isotopied into the next by elementary moves on the ribbon. These moves cannot change the knot type of the center polygon and the local algorithm is reducible. Consequently, if R_0 is a ribbon of knot type T, then the ergodicity class $\varepsilon(R_0)$ is a set of ribbons all with knot type T. We shall prove that the ergodicity classes are those sets of ribbons with fixed knot type of the center polygon.

Before giving the technical details of the proof characterizing the ergodicity classes, we give a sketch outlining the proof. The basic idea is to focus on a projection in a plane of a polygon derived from the ribbon. We show that Reidermeister moves can be executed on this polygon, using moves from the list of local ribbon moves. To do this, one needs to be able to create space around the ribbon, and this is accomplished by a process of successive subdivision of the ribbon. This is similar in spirit to the proof that the BFACF algorithm for polygons in Z^3 has knot types as its ergodic classes.

Notation. Let α be one of the canonical unit vectors $\{\pm i, \pm j, \pm k\}$ in $\mathscr{Z}^3$. A plaquette σ is *normal* to α if the cross-product of any pair of perpendicular edges of σ is parallel or antiparallel to α. Otherwise, we say that σ is *tangent* to α. An edge in $\mathscr{Z}^3$ can be represented by the double (x, α) with endpoints x and $x+\alpha$. Similarly, a plaquette can be represented by the triple (x, α_1, α_2), where $\alpha_1 \perp \alpha_2$ and with vertices x, $x+\alpha_1$, $x+\alpha_2$, and $x+\alpha_1+\alpha_2$. The *plane* $T_\alpha(x) \subset \mathscr{R}^3$ is normal to α and contains the points x. A *cut* of a ribbon R by $T_\alpha(x)$ is the intersection $R \cap T_\alpha(x)$. A *section* of a ribbon R is a connected sequence of plaquettes. A section is in *standard form* if its projection in a plane is a set of edges (containing no plaquettes). A section is *planar* if it is confined to the subspace between the plane (*including*) $T_\alpha(x)$ and the plane (*excluding*) $T_\alpha(x+\alpha)$(this plane may contain edges from the section, but not plaquettes); we say that the section is *planar with respect to* $T_\alpha(x)$. We also define the following half-spaces: Let $Z_\alpha^+(x) = \{z \in \mathscr{R}^3 \mid z = y + q\alpha,\ y \in T_\alpha(x),\ q \geqslant 0\}$ be the closed half-space with boundary $T_\alpha(x)$. Let $Z_\alpha^-(x) = \mathscr{R}^3 - Z_\alpha^+(x)$ be the open half-space with

boundary $T_\alpha(x)$. We denote by $S+\alpha$ the image of the set S if it is translated by the vector α.

Definition. Let R be a ribbon and let $R_+ = Z_\alpha^+(x+\alpha) \cap R$ and $R_- = Z_\alpha^-(x \cap R$. Let $(R_+ - \alpha)$ be the image of the set R_+ translated by $-\alpha$. If $R' = (R_+ - \alpha) \cup R_-$ is a ribbon, and if the number of plaquettes of R' equals the number of plaquettes in R minus the number of sections in R^+ and R^-, then R is *subdivided* by $T_\alpha(x)$.

Observations:

1. The condition on the number of plaquettes in R' in the above definition ensures that only single plaquettes tangent to α between the planes $T_\alpha(x)$ and $T_\alpha(x+\alpha)$ were contracted to give R', translating all of R^+ by $-\alpha$.

2. A subdivision R' of a given ribbon R can be constructed as follows: Let $R^+ = Z_\alpha^+(x) \cap R$ and $R^- = Z_\alpha^-(x) \cap R$. We can transform $(R^+ + \alpha) \cup R^-$ into a ribbon R' by adding single plaquettes to reconnect the ribbon edges divided by translating R^+.

3. If a sequence of such subdivisions connects a ribbon R to a ribbon R', then one says that R' is a subdivision of R.

4. Observe that every section of a ribbon subdivided by the plane $T_\alpha(x)$ between $T_\alpha(x)$ and $T_\alpha(x+\alpha)$ is a single ordinary plaquette with ribbon edges in $T_\alpha(x)$ and $T_\alpha(x+\alpha)$, and that no plaquette normal to α remains in $T_\alpha(x)$ [since $Z_\alpha^+(x)$ is a closed half-space in item 2 above].

5. Let S be a planar section of a ribbon R with respect to $T_\alpha(x)$. The end edges of S are those ribbon edges of R incident on plaquettes in S and R/S. Suppose that the end edges of S are incident with plaquettes η and τ in R/S. Then η and τ are plaquettes either in $Z_\alpha^+(x+\alpha)$ or in $Z_\alpha^-(x)$. If η or τ are *ordinary* plaquettes whenever they are in the half-space $Z_\alpha^+(x+\alpha)$, then S is called a *movable planar section.*

Standard Planar Sections. A section S of a ribbon is in standard planar form if it is planar with respect to some plane $T_\alpha(x)$ and if its projection in that plane is a set of edges. Standard planar sections have the following properties:

1. Each standard planar section of length N consists of the end plaquettes which are corner plaquettes, and $N-2$ internal plaquettes which are all ordinary.

2. 90° rotations may be used to transform a standard planar section into any other standard planar section connecting the same end vertices: To see this, consider the projected image of the section as a self-avoiding

walk. If one can perform BFACF algorithm moves on this projected walk by performing 90° rotations in the section, then the irreducibility of the BFACF algorithm in two dimensions immediately implies the claim[15, 16] (the elementary moves of this algorithm are illustrated in Fig. 6). This can be easily checked: Let $\sigma=(x, \alpha, \alpha_1)$ be an internal plaquette, and let $\eta=(x, \alpha\mu)$ and $\tau=(x+\alpha_1, \alpha, \nu)$ be its adjacent plaquettes in the section. Perform two 90° rotations on σ: first around the edge (x, α_1) to (x, α_1, α_2) and then around $(x+\alpha_2, \alpha_1)$ to $(x+\alpha_2, \alpha, \alpha_1)$. If $\mu=\nu=\alpha_2$, then η and τ are deleted, giving the type -2 move in Fig. 6. If $\mu\neq\alpha_2$ and $\nu\neq\alpha_2$, then the type $+2$ move in Fig. 6 is found. Otherwise, either $\mu=\alpha_2$, or $\nu=\alpha_2$ in which case the type 0 move is obtained.

3. Any subsection of a standard planar section may be translated normal to $T_\alpha(x)$ by applying parallel shifts; and if an end plaquette is included in the subsection, by doing corner moves. Since each move is reversible, any standard section which projects to a self-avoiding walk in $T_\alpha(x)$ may be made planar by using parallel shifts and corner moves.

Lemma 3.1. Let S be a movable planar section of a ribbon R with respect to the plane $T_\alpha(x)$. Suppose that S consists of more than one plaquette. If every ribbon edge of the translated image $S+\alpha$ is disjoint with R/S, except for the end edges, which may intersect R/S only in it first and last plaquettes, then elementary moves can be used to translate S onto its translated image $S+\alpha$, provided that corner moves, 90° rotations, parallel shifts, and double moves are included in the list of available elementary moves, generating a new ribbon with S translated by α.

Proof. If $y\in T_\alpha(x+\alpha)$ is a vertex occupied by S, then $y-\alpha\in T_\alpha(x)$ is also occupied by S. Let σ be a plaquette in S and let η and τ be plaquettes incident with σ and η' and τ' be second nearest neighbors of σ. The strategy is to rotate every plaquette σ in S tangent to α, using only vertices occupied by σ or by $\sigma+\alpha$. There are two cases to consider: Any normal plaquette may be either a corner plaquette or an ordinary plaquette. There are several subcases in each case.

Case (1). Suppose that σ is a normal, corner plaquette. The subcases are determined by the orientations and nature of η and τ. Let

Fig. 6. The BFACF moves.

$\sigma=(x, \alpha_1, \alpha_2)$, $\eta=(x, \alpha_1, \mu)$, and $\tau=(x, \alpha_2, \nu)$ Here, μ and ν may each independently take on three values, but many of them are identical under exchange of η and τ. Moreover, the only case which has $\mu=\nu$ is when η and τ are normal to α. There are four subcases left: (μ, ν) equal to (a) $(\alpha, -\alpha)$, (b) $(-\alpha_2, -\alpha_1)$, (c) $(\alpha, -\alpha_1)$, and (d) $(-\alpha_2, -\alpha)$:

Subcase (a). η' is disjoint with the edge (x, α), since there are already three plaquettes incident on x. Observe that $x+\alpha$ can only be incident on two plaquettes, since S is a movable planar section. Perform a corner move of σ to rotate it to (x, α, α_2). Then σ has become tangent to α.

Subcase (b). Perform a double move on σ and one neighbor, say η in the direction α. This move introduces two new ordinary plaquettes between σ and τ, (x, α, α_2), and between η and η', both tangent to α. If η is a corner plaquette, then the corner move which rotates σ from $(x+\alpha, \alpha_1, \alpha_2)$ to (x, α, α_1) followed by a second corner move which takes η from $(x+\alpha, \alpha_1, -\alpha_2)$ to $(x+\alpha_1, \alpha, -\alpha_2)$ rotate both σ and η tangent to α. On the other hand, if η is an ordinary plaquette, then a corner move of σ from $(x+\alpha, \alpha_1, \alpha_2)$ to (x, α, α_1) followed by a 90° rotation of η around $(x+\alpha, -\alpha_2)$ to $(x, \alpha, -\alpha_2)$ leaves both σ and η tangent to α.

Subcase (c). This case is dealt with exactly as in subcase (a).

Subcase (d). This case is treated exactly as in subcase (b).

Case (2). Suppose that σ is a normal, ordinary plaquette. This case has two subcases: Either η or τ or both are normal to α, or neither are.

Subcase (a). Suppose either η or τ or both are normal to α; without loss or generality, suppose it is η. Perform a double move on σ and η and argue exactly as in case (1), subcase (b).

Subcase (b). Neither η nor τ is normal to α. Let $\sigma=(x, \alpha_1, \alpha_2)$, and suppose that $\eta=(x, \alpha_1, \mu)$ and $\tau=(x+\alpha_2, \alpha_1, \nu)$, where μ and ν are $\pm\alpha$. If either μ or ν, or both, are equal to α, suppose without loss of generality that $\mu=\alpha$. Then the vertices $(x+\alpha)$ and $(x+\alpha_1+\alpha)$ are incident on at most two plaquettes (each) by hypothesis, and either $(x+\alpha_2)$ or $(x+\alpha_1+\alpha_2)$ is incident on only two plaquettes. In the first case rotate σ by a 90° rotation tangent to α about (x, α_2), introducing the plaquette $(x+\alpha_2, \alpha, \alpha_1)$ if necessary between σ and τ, or deleting τ. In the second case, σ is rotated though 90° about its other boundary edge $(x+\alpha_1, \alpha_2)$ to $(x+\alpha_1, \alpha, \alpha_2)$. In both cases σ is rotated tangent to α. On the other hand, if both μ and ν equal $-\alpha$, then S consists of exactly one plaquette, and this case is not covered by our hypothesis (we will remove these from the ribbon by applying the result in Corollary 3.2 and Lemma 3.3).

Consider every plaquette in S normal to α, and systematically rotate each one tangent to α. Each possible case is covered above, since S has length greater than one. Consequently, S is transformed into S_T, a planar section standard with respect to $T_\alpha(x)$. Now, S_T has exactly two corner plaquettes at its endpoints, and all its internal plaquettes are ordinary. Moreover, each vertex covered by S_T is either in S or in $S+\alpha$.

Suppose that σ is an internal plaquette tangent to α in $S+\alpha$. By remark 2 on standard planar sections, 90° rotations may be used to arrange S_T such that $\sigma-\alpha$ is an internal plaquette in S_T. If σ is an ordinary plaquette, then a parallel shift of $\sigma-\alpha$ by α will create σ as well as its tangent neighbors in $S+\alpha$ (observe that the neighbors of σ must be tangent to α if σ is ordinary). These moves are possible since $S+\alpha$ is internally disjoint with R/S by the hypothesis. If there are no internal plaquettes in $S+\alpha$, then S has length two, and a single corner move will translate it by α. Consequently, it only remains to rotate the remaining tangent plaquettes in S_T to their normal images in $S+\alpha$: But this is always possible, since these cases can be considered as rotating plaquettes from normal to tangent by rotating the frame of reference. Thus S has been translated to $S+\alpha$. ▮

The case analysis in Lemma 3.1 detected the only case where a planar section is always movable and consists of exactly one plaquette [say with respect to $T_\alpha(x)$]: We refer to this single case as a *degenerate section.* By elimination, one observes that this section has exactly one ordinary plaquette (normal to α), and has neighboring plaquettes η and τ tangent to α in the half-space $Z_\alpha^-(x)$. One also observes that any planar section of a ribbon R which satisfies the conditions of Lemma 3.1 may be rotated, plaquette by plaquette, to a standard planar section; that is, its image in $T_\alpha(x)$ will be a self-avoiding walk.

Corollary 3.2. The only movable planar section with respect to the plane $T_\alpha(x)$ which contains exactly one plaquette (x, α_1, α_2) is an ordinary plaquette normal to α with neighboring plaquettes η and τ tangent to α in the half-space $Z_\alpha^-(x)$.

Degenerate sections can be removed from a ribbon by using 90° rotations: consequently, every ribbon is equivalent to a ribbon without degenerate sections under 90° rotations. One may therefore restrict the discussion to ribbons without degenerate sections; we call these ribbons *free*:

Lemma 3.3. By applying 90° rotations, a movable planar section with respect to the plane $T_\alpha(x)$ containing exactly one plaquette can be removed from any ribbon.

Proof. Let $\sigma=(x,\alpha_1,\alpha_2)$ be the movable planar section; then by Corollary 3.2, the neighbors of σ are $\eta=(x,\alpha_2,-\alpha)$ and $\tau=(x+\alpha_1,\alpha_2,-\alpha)$. σ is an ordinary plaquette, and there are two cases to consider: case (1) when both η and τ are ordinary plaquettes, and case (2) when at least one of η and τ is a corner plaquette.

Case (1). In this case, $(x-\alpha,\alpha_2)$ and $(x+\alpha_1-\alpha,\alpha_2)$ are ribbon edges. Rotate σ by 90° to $(x,\alpha_1,-\alpha)$ around (x,α_1), and then again around $(x-\alpha,\alpha_1)$ to $(x-\alpha,\alpha_1,\alpha_2)$. This deletes the plaquettes η and τ from the ribbon. No other vertices other than those initially occupied by η and τ were used. Rename the current neighbors of σ to be η and τ again. If both are ordinary plaquettes, then case (1) is again encountered, and the construction is repeated, again translating σ by $-\alpha$. Since the ribbon is finite, one must eventually encounter case (2).

Case (2). Without loss of generality, suppose that η is a corner plaquette incident on the second nearest neighbor $\eta'=(x,-\alpha,-\alpha_i)$, where $i=1$, or 2. As in case (1), perform a 90° rotation of σ around (x,α_1) to $(x,\alpha_1,-\alpha)$. This removes η. If case (1) or case (2) is again encountered, then the constructions are repeated. Since in both cases plaquettes are removed from the ribbon and never added, σ must eventually become part of a planar section with length greater than one. ∎

Hence, our attention will be restricted to free ribbons; by Lemma 3.3, there exists a sequence of 90° rotations between any ribbon and a free ribbon. It is now possible to show that any free ribbon may be subdivided in any given plane, using elementary local moves from the lists in Section 3.1.

Theorem 3.4. Let R be any free ribbon, and let R' be obtained by subdividing R with respect to the plane $T_\alpha(x)$, where $x\in\mathscr{Z}^3$. Then there exists a sequence of elementary moves which transform R into R', provided that corner moves, parallel shifts, 90° rotations, and double moves are included in the set of possible elementary moves.

Proof. Without loss of generality, suppose that $T_\alpha(x)\cap R\neq\varnothing$. Let j be the largest integer such that $T_\alpha(x+j\alpha)\cap R\neq\varnothing$. Suppose R contains planar sections with respect to $T_\alpha(x+j\alpha)$, and let S be any one such planar section. Since R is free and $S+\alpha$ is disjoint with R/S, S satisfies the hypothesis of Lemma 3.1, and consequently there exists a sequence of elementary moves which will translate S by α onto $S+\alpha$. If any planar sections with respect to $T_\alpha(x+j\alpha)$ remain, then these also satisfy the hypothesis of Lemma 3.1, and they are also translated by α. Continue until none remains, then R is subdivided in the plane $T_\alpha(x+j\alpha)$. Observe that only plaquettes tangent to α were added at the endpoints of each of the translated sections.

If $j=0$, then the theorem is proven, so suppose that $j \geqslant 1$. Reduce j by 1 and look for planar sections in R with respect to $T_\alpha(x+j\alpha)$. If S is such a section, then it satisfies the hypothesis of Lemma 3.1, since R is free and since R has been subdivided in $T_\alpha(x+(j+1)\alpha)$. In addition, the end edges of $S+\alpha$ can only be incident on the end plaquettes of R/S. Thus S can be translated by α. Continue until every planar section with respect to $T_\alpha(x+J\alpha)$ has been translated. Then R has been subdivided in $T_\alpha(x+j\alpha)$. If $j=0$, then the theorem is proven; otherwise reduce j by 1 and repeat. Finally, $j=0$.

Observe that a subdivision of a free ribbon is also free. A free ribbon R can be subdivided multiple times in any number of planes, not all necessarily with the same orientation. Consequently, a natural consequence of Theorem 3.4 is as follows.

Corollary 3.5. Let R be any free ribbon, and let R' be the ribbon obtained by subdividing R multiple times. Then there exists a sequence of local elementary moves which includes corner moves, parallel shifts, 90° rotations, and double moves, which when applied to R, gives R'. In addition, R' is a free ribbon.

If a free ribbon R is subdivided systematically in every plane $T_\alpha(x)$ which cuts it, and for α assuming all the canonical unit vectors, to give a free ribbon R', then R' is said to be *globally subdivided.* By Corollary 3.5, every ribbon (not necessarily free) is connected to a globally subdivided free ribbon by a sequence of elementary moves.

By applying the arguments in Lemma 3.1, any planar segment in a globally subdivided ribbon can be changed into a standard planar segment, all with respect to a plane $T_\alpha(x)$. Thus, we can transform any ribbon R into a standard ribbon: the image of R in $T_\alpha(x)$ under a projection in the direction α is a set of edges.

Corollary 3.6. Let R be an arbitrary ribbon. By applying an elementary transition from a list which includes corner moves, parallel shifts, 90° rotations, and double moves, R can be changed into a standard ribbon with respect to any given plane $T_\alpha(x)$.

Canonical Standard Ribbons. Let R be a standard ribbon with respect to $T_\alpha(x)$. Let $\mathscr{P}R$ be the projection of R into $T_\alpha(x)$. If e is an edge in $\mathscr{P}R$, then e is the image (under $\mathscr{P}$) of at least one plaquette in R. The number of plaquettes projected to e may be determined by making slight changes in α, and these may contain, in addition to internal (ordinary) plaquettes of standard planar sections, also linear connected sections of plaquettes (all with the same orientation) vertical to $T_\alpha(x)$. Denote these

sections as *vertical sections.* A vertical section consists of two terminal plaquettes which are both corner plaquettes, and which are also the terminal plaquettes of standard planar sections, as well as internal ordinary plaquettes. Two vertical sections are adjacent if a terminal (corner) plaquette of each forms a standard planar section of length two. In this manner, one may consider a standard ribbon to consist of a collection of vertical sections glued together by planar sequences of (ordinary) plaquettes (which may be empty), and which together with the terminal plaquettes of the adjacent vertical sections form a standard planar section in R. A vertical section S is *included* if it is incident on R/S on opposite sides of S (this is well defined, since every plaquette in S has the same orientation), otherwise it is *excluded.* If R is globally subdivided, then S is movable, and by Remark 2 on standard planar sections and Lemma 3.1, any excluded vertical section S may be translated and be changed into an included vertical section. [To see this, argue as follows: Let $\eta = (x, \alpha, \alpha_1)$ and $\tau = (z + k\alpha, \alpha, \alpha_2)$ be the two plaquettes adjacent to an excluded vertical section S. One may assume that η and τ have the same orientation; if not, then subdivision and translation of S in the direction away from its incident plaquettes will introduce two new plaquettes of the same orientation. Thus $\alpha_1 = \alpha_2$ above. If η has the same orientation as S, then two 90° rotations (after subdivision if necessary) will introduce a plaquette adjacent to S rotated at 90° with S, so one may assume that η is rotated 90° with respect to S. Thus, the terminal plaquette of S incident on η is of the form (x, α, α'), where $\alpha \neq \alpha' \neq \alpha_1$. Consequently, two 90° rotations of η will translate it to $(x + \alpha', \alpha, \alpha_1)$, and this is incident on the opposite side of S to τ] If every vertical section of a standard ribbon R is included, then R is said to be in *canonical standard form.* Consequently, we have just shown that:

Lemma 3.7. Any standard ribbon R may be put in canonical standard form by using elementary transitions from a list that includes corner moves, parallel shifts, 90° rotations, and double moves.

Polygons and Ribbons. It may also be arranged that every edge e in the image $\mathscr{P}R$ of a ribbon in canonical standard form is projected from either an included vertical section or from an internal ordinary plaquette in a planar standard section of R, using subdivision and pushing planar sections onto newly introduced planes perpendicular to $T_\alpha(x)$. In such a projection, every intersection occurs on vertices, and by indicating the nature of the intersections, the projection may be interpreted as that of a polygon. Consequently, one may "lift" the projection to either the ribbon or to a polygon. BFACF moves in the polygon induce BFACF moves in the projection, which in turn induce local moves from our list of available moves

in the ribbon. Subdivision of the polygon is possible with BFACF moves, and such a subdivision induces a similar subdivision in the ribbon. Note that the ribbon has the same knot type as the lifted polygon. A theorem of Janse van Rensburg and Whittington[17] implies that by subdivision and by BFACF moves, any polygon of knot type T may be changed such that its projection is a plane isotopy of a standard projection of a knot of type T (for example, that projection listed in the standard knot tables). Moreover, if the standard knot projection is pushed onto the lattice, then the projection of the polygon may be made identical to it. Intersections in the projection $\mathscr{P}R$ may be identified to have overpassing and underpassing sections. From underpass to underpass, a projected section is a self-avoiding walk, and by using parallel shifts the corresponding section can be made planar. Hence, the entire ribbon can be made planar, except for underpasses which must avoid overpassing sections. BFACF moves in the polygon lifted from the projection of this ribbon induce ribbon moves; the involved section is first made planar, and collisions are avoided by parallel shifts normal to $T_\alpha(x)$. Consequently, R may be changed into a ribbon with identical projection to that of a standard projection $\mathscr{P}P_T$ of a polygon of knot type T, as discussed above. Taken together, any canonical standard ribbon may be changed into a ribbon R such that $\mathscr{P}R = \mathscr{P}P_T$, provided that R has knot type T. But since any ribbon may be made into a ribbon in canonical standard form, one obtains:

Theorem 3.8. The ergodicity class $\mathscr{E}(R_0)$ of the ribbon algorithm initialized with ribbon R_0 of knot type $K(R_0)$ is

$$\mathscr{E}(R_0) = \{R \in \mathscr{R} \mid K(R) = K(R_0)\}$$

where $K(R)$ is the knot type of ribbon R.

Corollary 3.9. The ribbon algorithm is reducible, and its ergodicity classes are those sets of ribbons with the same knot type.

3.3. Irreducibility and Non local Moves

By Corollary 3.9 it is apparent that moves additional to the lists in Section 3.1 are needed to define an irreducible Monte Carlo algorithm on the set $\mathscr{R}$ of ribbons in three dimensions. The simplest remedy is the inclusion of a "crankshaft" move, as suggested in the case of the BFACF moves.[18] This type of move is illustrated in Fig. 7, and one may imagine it as a point reflection of the section of the ribbon through the center of mass of the marked ribbon edges.

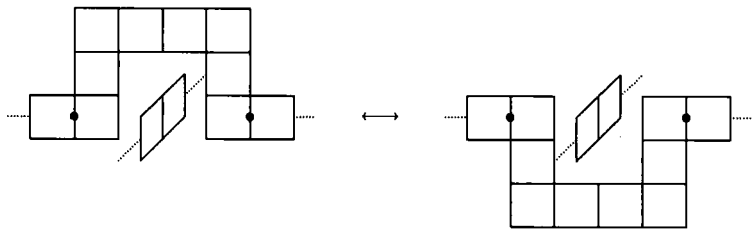

Fig. 7. A. crankshaft move. This move may also be achieved by reflecting the section between the marked ribbon edges through the center of mass of the midpoints of the edges.

The proposed crankshaft moves, together with subdivisions if necessary, can be used to "untie" any knotted polygon, and since the ribbon algorithm is ergodic if applied to unknotted polygons, the augmented algorithm (with added crankshaft moves) is irreducible. It was already observed that crankshaft moves may be achieved by performing point reflections on sections with end edges which are parallel. Borrowing from the literature on the simulation of polygons, this move can be identified as a "pivot" move, and may be generalized as follows: With uniform probability, select two distinct ribbon edges and find the shorter section of the ribbon between these. If the ribbon edges are not parallel, then reject the attempt; otherwise, perform a point reflection of the section through the center of mass of the selected ribbon edges; this guarantees that the ribbon edges are interchanged. If the resulting structure is a ribbon, then accept the attempt; otherwise reject it. Since these moves leave the length of the ribbon unchanged and are reversible, they do not upset the detailed balance equation (3.2) in Section 3.2. Taken together we obtain the following result:

Theorem 3.10. If a list of local moves which includes corner moves, parallel shifts, 90° rotations, and double moves applied to a ribbon is augmented by the addition of either a crankshaft move or by a pivot, then the resulting Monte Carlo algorithm is irreducible.

4. IMPLEMENTATION OF THE ALGORITHM

The algorithm described in Sections 2 and 3 consists of both local moves (which change the geometry and number of plaquettes in a local area) and global moves (which change the geometry of potentially large segments of the ribbon). In order to implement these moves efficiently in

a computer, one must design data structures which may be manipulated efficiently if a move is attempted. The basic structure in a ribbon is a plaquette, which cannot be described by simply storing a d-dimensional array of integer coordinates—the plaquette has an orientation, and its adjacency to other plaquettes is through its edges. We therefore encoded each plaquette in a structure called a *face*, which contains the following information:

1. The bottom southwest vertex v_{bsw} of the plaquette, as a three-dimensional integer array.

2. A character variable c_O, which describes the orientation of the plaquette: it may take one of three values, XY, YZ, or ZX.

3. Four equal substructures, one for each edge in the plaquette. Each substructure codes the coordinates of the vertices at the ends of an edge. We also grouped these into two pairs; the first pair contains the ribbon edges of the plaquette, and the second pair the boundary edges. These data are redundant, since one may compute them from v_{bsw} and c_O; nevertheless, these were helpful in performing geometric checks other than self-avoidance in the implementation.

A structure for storing the ribbon is constructed from *faces* as a contiguously allocated, unordered, doubly linked list of pointers called a *ribbon*. Each pointer in the list is the address of a face structure, and points to that location in memory which stores the structure of a particular face. In order to keep track of the sequence of plaquettes in the ribbon, the structure *face* is made *doubly self-referential*; two pointers are added to it which point to the structure *face* itself. One pointer gives the address of the next plaquette in the ribbon, and the other points to the previous plaquette in the ribbon. We refer to these as the *forward* and *backward* pointers, respectively. Since the ribbon is closed, each plaquette has a forward and a backward pointer.

The ribbon is also self-avoiding, and we used hash-coding[19] with linear probing in order to check self-avoidance during an attempted move. This is a particularly useful technique. Most queries and operations in the hash-table may be done in $O(1)$ CPU time, provided that there are not too many collisions in the hash-table. We simply hashed all the vertices in the lattice which were occupied by the ribbon, and these were updated every time a move was accepted by the algorithm.

The basic operations on our data structures involved the following actions: (1) selecting an edge or a plaquette with uniform probability from the ribbon, (2) changing the orientation of a plaquette, (3) inserting

one or two new plaquettes into the ribbon, and (4) removing one or two plaquettes from the ribbon. The ribbon changes length as the algorithm is applied, so we used dynamically allocated arrays: inserting new data results in the allocation of new memory, and removing data results in the release of previously allocated memory. The advantage is that we do not have to predict a maximum length before a run and risk writing outside an array. Selecting a plaquette with uniform probability is easily achieved by choosing a pointer in the ribbon structure with uniform probability. Similarly, a ribbon edge may be selected with uniform probability by first selecting a plaquette and then selecting one of its ribbon edges with uniform probability. Elementary transitions are proposed and then subjected to three tests: the newly proposed ribbon must be self-avoiding, have no more than three plaquettes incident on the same vertex, and be accepted with a Metropolis-style implementation. All these tests can be done locally for local moves; in the case of nonlocal moves, one simply checks around the pivot points for violations of self-avoidance.

4.1. Implementing Local Elementary Transitions

The local moves are all combinations of the following operations:

1. Change the position and orientation of a plaquette. In this case one simply updates the data structures which code the relevant information. These are the hash-table and the structure *face*.

2. Remove a plaquette. The corresponding structure *face* which coded the plaquette is freed, and the neighboring plaquettes must have their forward and backward pointers updated. In addition, we remove the pointer which points to the plaquette from the ribbon structure. In addition, we remove the vertices of the plaquette from the hash-table. The length of the ribbon is decreased by 1.

3. Insert a new plaquette. Here we add a pointer to the ribbon structure, allocate memory for a face structur to code the position, orientation, and forward and backward pointers of the new plaquette, and add its vertices to the hash-table. The length of the ribbon is increased by 1.

The transition probability from a ribbon R_1 to a ribbon R_2 via an elementary move was computed in Section 3 as

$$\text{Prob}\{R_1 \to R_2\} = \frac{A(\mathcal{M})}{|R_1|} \begin{cases} 1 & \text{if } |R_1| \geq |R_2| \\ K^{|R_2|-|R_1|} & \text{otherwise} \end{cases} \tag{4.1}$$

where $A(\mathcal{M})$ is a function of the type of move $\mathcal{M}$ attempted. We verified that (4.1) implies the detailed balance condition

$$\pi(R_1)\,\mathrm{Prob}\{R_1 \to R_2\} = \pi(R_2)\,\mathrm{Prob}\{R_2 - R_1\} \tag{4.2}$$

for all ribbons R_1, R_2, where the invariant limit distribution is given by

$$\pi(R) = \frac{K^{|R|}\,|R|}{G_1(K)} \tag{4.3}$$

where $G_1(K)$ normalizes $\pi(R)$ and is the generating function of the ribbons. We define the κ-generating function as

$$G_\kappa(K) = \sum_R K^{|R|}\,|R|^\kappa \tag{4.4}$$

In order to sample from $G_\kappa(K)$ we introduce two Monte Carlo filters. The first filter is defined by

$$p_1 = \frac{|R_1|}{|R_1| + |R_2|}$$

That is, if R_2 is obtained from R_1 by an elementary move, then *reject* the move with probability $1 - p_1$. If the move is not rejected, then it has passed through the first filter. The second filter is then encountered, and it is determined by

$$p_2 = \begin{cases} \dfrac{|R_2|^\kappa}{|R_1|^\kappa + |R_2|^\kappa}\,K^{|R_2| - |R_1|} & \text{if} \quad |R_2| > |R_1| \\ \dfrac{|R_2|^\kappa}{|R_1|^\kappa + |R_2|^\kappa} & \text{otherwise} \end{cases} \tag{4.5}$$

The move is rejected with probability $1 - p_2$, otherwise it passes through this filter as well. The probability for passing through both filters is thus $p_1 p_2$ (provided that R_2 is a ribbon), and this is given by

$$\mathrm{Prob}\{R_1 \to R_2\} = A(\mathcal{M}) \begin{cases} B(R_1, R_2)\,|R_2|^\kappa & \text{if} \quad |R_1| \geqslant |R_2| \\ B(R_1, R_2)\,|R_2|^\kappa\,K^{|R_2| - |R_1|} & \text{otherwise} \end{cases} \tag{4.6}$$

where

$$B(R_1, R_2) = B(R_2, R_1) = \frac{1}{|R_1| + |R_2|} \frac{1}{|R_1|^\kappa + |R_2|^\kappa} \tag{4.7}$$

The detailed balance derived from (4.6) implies an invariant limit distribution given by

$$\pi(R) = \frac{K^{|R|} |R|^\kappa}{G_\kappa(K)} \tag{4.8}$$

or we simply say that sampling is from $G_\kappa(K)$. The parameter κ is an input parameter in the algorithm, and we may fix it to suit our purposes in any simulation.

4.2. Implementation of Global Moves

Global moves on segments of a ribbon may come in a wide variety of possibilities determined by the elements of the octahedral group.[19] We limit outselves here to one of these, called an *inversion*, which is a point reflection of a segment (of a ribbon) though the center of mass of two "pivots" which were picked subject to some constraints (which we will explain later). Other types of moves may be implemented in a similar manner. The pivots which we choose in a ribbon may either be edges or plaquettes; in the description of global moves in Section 3 we only used edges as pivots, but that is now generalized to include plaquettes as well.

A global move is performed by first selecting two plaquettes (p_1 and p_2) in the ribbon with uniform probability. If these are neighbors, then we do the null move; otherwise the plaquettes separate the ribbon into two segments. A global move is attempted on the shorter of the two. In addition, we find those ribbon edges incident on the selected plaquettes and shared with the shorter segment of the ribbon; call these e_1 and e_2. If p_1 and p_2 have the same orientation, then an inversion of the shorter ribbon segment through their center of mass may be attempted. If the resulting object is a ribbon, then the move is accepted. On the other hand, if the edges e_1 and e_2 may be attempted, and if the resulting object is a ribbon, then the move is accepted. Implementation of these cases is as follows:

1. If p_1 and p_2 have different orientations and e_1 and e_2 are perpendicular, then no global move is possible, and we reject the attempt.

2. If p_1 and p_2 are oriented the same way, but e_1 and e_2 are perpendicular, then an inversion through the center of mass of p_1 and p_2 is attempted.

3. If p_1 and p_2 are differently oriented, but e_1 and e_2 are parallel, then an inversion through the center of mass of e_1 and e_2 is attempted.

4. Otherwise, if both p_1 and p_2 have the same orientation, and e_1 and e_2 are parallel, then we may attempt either; they are equivalent.

Let the shortest piece of the ribbon be the ordered sequence $\{p_i\}_{i=1}^{m+1}$ of plaquettes, where p_0 and p_{m+1} are the plaquettes chosen uniformly from all the plaquettes. Let $\mathbf{v}_j(i)$ be the position vector of the ith vertex of the plaquette p_j. Moreover, let the position vectors of the midpoints of the pivots (either the plaquettes or edges described in the two cases above) be $\mathbf{w}_1$ and $\mathbf{w}_2$. Then the reflected images though the center of mass of the pivots of the position vectors of the vertices are

$$\mathbf{v}'_j(i) = \mathbf{w}_1 + \mathbf{w}_2 - \mathbf{v}_j(i), \qquad \text{where} \quad i = 1,..., m; \quad j = 1,..., 4 \tag{4.9}$$

This move exchanges the order of the plaquettes in the shorter segment of the ribbon, and the pointers at p_0 and p_{m+1} must be updated if it is successful. In order to check effectively self-avoidance, we used a scratch hash-table. We read the vertices of the ribbon, starting at the pivots and alternating between them, into the scratch hash-table. If an intersection is encountered, then the move is rejected, and the scratch hash-table is cleared. Otherwise, the whole ribbon is hashed into the scratch hash-table and we interchange the scratch hash-table with the original hash-table, which is cleared instead. The pointers in the ribbon structure are updated if the move is successful, to account for the reversal in the order of the plaquettes in the shorter segment.

5. NUMERICAL TESTING AND RESULTS

The data structures described in Section 4 are conveniently implemented in C. The algorithm was coded and set of initial runs was performed to determine the numerical properties of the algorithm. Initial bias was dealt with typically by discarding the first T iterations in any simulation, where T is large and dependent on the fugacity K and the input parameter q. A magnitude for T may be guessed by computing the exponential autocorrelation time $\tau_{\text{exp}}(A, K)$ for various global metric properties A of the ribbon and for various values of K. If $\tau^*(K) = \max_A(\tau_{\text{exp}}(A, K))$, then T was taken as $10\tau^*(K)$(and the maximum over A is taken over the limited

number of properties we computed). Our runs were initialized by a planar ring of plaquettes, and we sampled once every 5×10^4 iterations. We selected q in Eq. (3.1) equal to 1/4, which implies that once every four attempts a double move is proposed, and p was put equal to 1/2 in Eq. (3.4), which means that parallel shifts and 90° rotations were selected uniformly if an ordinary plaquette is chosen. Nonlocal moves were performed randomly on average about once every $\langle n \rangle/4$ moves. The parameter κ in the generating function was put equal to 3 by tuning it in Eq. (4.5). This will bias the simulation to slightly higher values of n.

5.1. Autocorrelations

Expected values of the observables of ribbons are estimated by taking averages over realizations of Markov chains in the space of ribbons. These Markov chains are correlated, and statistical errors may be estimated for the averages only if the autocorrelation times of the observables under question are known. The autocorrelation time of an observable A may be estimated by using a natural estimator[20] for the integrated autocorrelation time over a realized Markov chain of length M:

$$\tau_{\text{int}}(A) = \frac{1}{2} \sum_{t=-(M-1)}^{M-1} \left(C_{AA}^{-1}(0) \frac{1}{M-|t|} \sum_{i=1}^{M-|t|} (A_i - \langle A \rangle)(A_{i+|t|} - \langle A \rangle) \right) \tag{5.1}$$

where $\langle A \rangle$ is the sample (or grand canonical) mean of the observable A which is measured after each iteration. In Eq. (5.1) we defined $C_{AA}(0) = \langle A^2 \rangle - \langle A \rangle^2$. The estimated integrated autocorrelation times may be used to compute an approximation to the statistical error in the Monte Carlo averages $\langle A \rangle$ by using the asymptotic formula

$$\sigma^2(A) \sim \frac{1}{M} [2\tau_{\text{int}}(A)] \, C_{AA}(0) \tag{5.2}$$

In other words, the variance $\sigma^2(A)$ of $\langle A \rangle$ is a factor $2\tau_{\text{int}}(A)$ larger than it would be if the realized sequence of observables A_i were statistically independent.

The integrated autocorrelation times for the number of plaquettes n and for the square radius of gyration S^2 of a ribbon (defined by locating unit masses at vertices in the ribbon) were estimated using Eq. (5.1). We list the results in Table I, where $\tau_{\text{int}}(A)$ for $A = n$ and $A = S^2$ were computed by running the algorithm at a variety of values for the fugacity K.

Table I. Measured Integrated Autocorrelation Times

Run length (cycles)	K	$\langle n \rangle$	$\tau_{int}(n)$	$\langle S^2 \rangle$	$\tau_{int}(S^2)$
1×10^9	0.2255	69 ± 2	13 ± 2	21.0 ± 1.0	12 ± 2
1×10^9	0.2260	77 ± 3	17 ± 2	24.0 ± 1.3	16 ± 3
2×10^9	0.2265	84 ± 4	22 ± 4	26.8 ± 1.6	20 ± 4
3×10^9	0.2275	97 ± 3	30 ± 4	32.1 ± 1.6	28 ± 4
5×10^9	0.2280	110 ± 4	42 ± 8	37.1 ± 1.9	39 ± 7
8×10^9	0.2285	127 ± 5	62 ± 14	44.7 ± 2.1	58 ± 14
10×10^9	0.2290	183 ± 13	183 ± 39	71.0 ± 7.0	179 ± 38
15×10^9	0.2295	252 ± 22	303 ± 75	104.6 ± 11.1	279 ± 69

It is not surprising that τ_{int} increases with K, and it seems to grow indefinitely as K approaches its critical value at $K_c = \rho^{-1}$. This is a typical feature of grand canonical Monte Carlo stochastic processes in the vicinity of a critical point. In particular, as $K \to K_c$, we argue like Caracciolo and Sokal[21] and conjecture the following scaling behavior for the integrated autocorrelation times:

$$\tau_{int}(A) \sim \langle \eta \rangle^{p_A} \tag{5.3}$$

where p_A is a critical exponent (describing the dynamics of the Monte Carlo process) which may be dependent on the observable A. The integrated autocorrelation time is related to statistical errors in averages by Eq. (5.2), so the rate of growth in (5.3) is a crucial factor in determining the statistical efficiency of the algorithm. A log–log plot of $\tau_{int}(A)$ against $\langle n \rangle$ is presented in Fig. 8, and the exponents were estimated by a two-parameter linear least squares fit:

$$\begin{aligned} p_n &= 2.51 \pm 0.08 \\ p_{S^2} &= 2.53 \pm 0.09 \end{aligned} \tag{5.4}$$

The local moves of the ribbon algorithm are analogous to moves in the BFACF algorithm for self-avoiding walks. In fact, the median of the ribbon undergoes changes which are BFACF-like, and the relaxation of a ribbon under the local moves will therefore be very similar to that of a walk undergoing BFACF moves. It is known that the exponential autocorrelation time of the BFACF algorithm is infinite for all values of the fugacity greater than 0,[22] and an argument similar to the argument in ref. 22 shows that the local ribbon algorithm also has an infinite

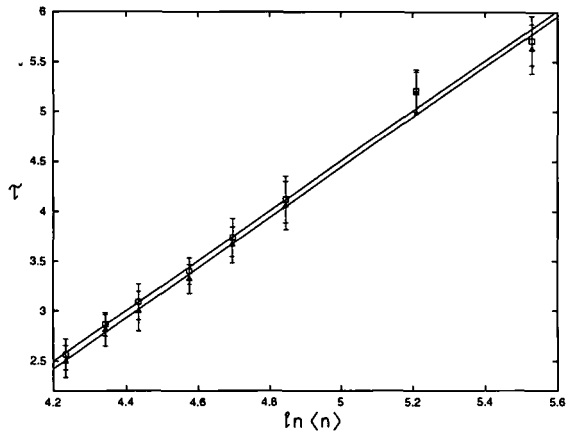

Fig. 8. Log–log plot of the autocorrelation time as a function of the plaquette fugacity K. The displayed data are for the length n of the ribbon (squares) and for the mean-squared radius of gyration $\langle S^2 \rangle$ (triangles).

exponential autocorrelation time. The integrated autocorrelation time of the BFACF algorithm appears to grow as

$$\tau_{\text{int}}(n) \sim \langle n \rangle^{4\nu} \tag{5.5}$$

where ν is the metric exponent of the walks.[23] The same argument implies that (5.5) should be true for ribbons as well, and we expect ν to have the same value for ribbons. In three dimensions, the occurrence of tight pseudoknots in the ribbon may increase the integrated autocorrelation times, perhaps even affecting the exponent in (5.5). The theoretical minimum in value of the dynamical exponent p_n is 2, from a random walk argument.[24] Our result of $p_n \sim 2.5$ is quite close to $4\nu \sim 2.4$. It is not clear whether the global moves affect the value of the exponent p_n; empirical evidence in self-avoiding walk studies suggests a decrease of a factor of 5–10 in integrated autocorrelation times.[25] These moves are crucial for ergodicity for closed ribbons, but also affect the dynamical behavior of the algorithm in a positive manner.

5.3. Estimation of ρ and α

Concatenation arguments may be used to prove a superadditive inequality for the number of closed ribbons: a direct result is that $r_n = \rho^{n+o(n)}$ and, in analogy with polygons, it is reasonable to expect that

$$r_n \sim n^{\alpha-3}\rho^n \tag{5.6}$$

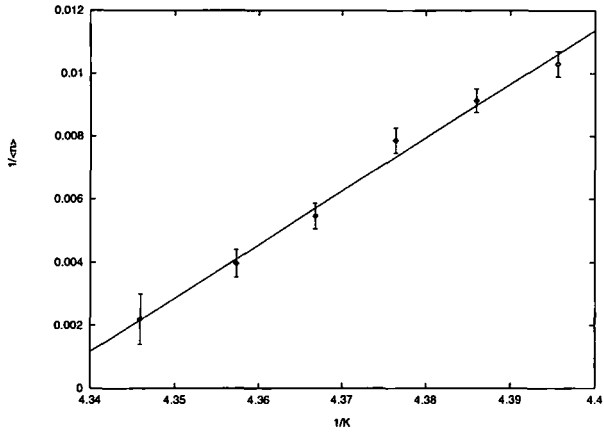

Fig. 9. Plot of $\langle n\rangle_\kappa^{-1}$ versus $1/K$ for $\kappa = 3$. In this analysis the intercept with the x axis gives ρ, while the estimate of α can be easily extracted from the slope of the fitted straight line.

ρ is the growth constant of both open and closed ribbons, and may be measured numerically through application of our algorithm. Theoretical bounds on ρ were give in Section 2: $4 \leqslant \rho \leqslant 9$.

The assumption (5.6) for r_n allows us to compute a scaling form for the generating function $G_\kappa(K)$ by simply substituting (5.6) into (2.3) and approximating the sum by an integral. At K_c, the generating function is singular, and its singular part diverges as K approaches $K_c(=1/\rho)$ as

$$G_\kappa(K) \sim \frac{\Gamma(\kappa+\alpha-2)}{\log(K_c/K)^{\kappa+\alpha-2}} \tag{5.7}$$

This estimate implies that the average number of plaquettes in the ribbon at K behaves like

$$\langle n\rangle_\kappa \sim \frac{K(\alpha-2+\kappa)\rho}{1-\rho K} \tag{5.8}$$

which is a simple pole in the K plane, and we should be able to compute both ρ and α by comparing this to our data. Consequently, we attempted a grand-canonical least-squares fit by plotting $1/\langle n\rangle_\kappa$ against $1/K$ (see Fig. 9).

The data appear to be well described by a linear relation. A weighted least squares fit using (5.8) gives

$$\begin{aligned} \rho &= 4.33 \pm 0.20 \\ \alpha &= 0.36 \pm 0.14 \end{aligned} \tag{5.9}$$

again with 95% confidence intervals propagated from the confidence intervals in the data (which we estimate from the fluctuations between independent runs). The estimate of ρ is consistent with the bounds $4 \leqslant \rho \leqslant 9$, and closer to the lower bound, and α is found to be within two standard deviations from its polygon value. The large confidence interval on α indicates strong corrections to scaling.

5.4. Estimation of ν

Let $S^2(R)$ be the square radius of gyration of the ribbon R. The ensemble average $\langle S^2(R) \rangle$ is expected to scale as

$$\langle S^2 \rangle_n \sim n^{2\nu} \tag{5.10}$$

as the number of plaquettes n tends to infinity, and where ν is a universal scaling exponent called the metric exponent. The asymptotic behavior in (5.10) can be written as an equality if hierarchies of confluent and analytic corrections are added, usually in the following way:

$$\langle S^2 \rangle_n = Bn^{2\nu}(1 + bn^{-\Delta} + \cdots) \tag{5.11}$$

ν may be estimated from data collected over realizations of ribbons for several values of K (in different runs). Let $N_K(n)$ be the number of ribbons of length n realized in a run with fugacity K. Let $\langle S^2(K) \rangle_n$ be the mean square radius of gyration over this sample. Then over all the runs (at various values of K) we compute

$$\langle S^2 \rangle_n = \frac{\sum_K N_K(n) \{ S^2(K) \rangle_n}{\sum_K N_K(n)} \tag{5.12}$$

which is a weighted average over the averages from the individual runs: the weights are proportional to the sample sizes. To compute ν we assume the scaling form

$$\langle S^2 \rangle_n = Bn^{2\nu}(1 + Cn^{-\Delta}) \tag{5.13}$$

ignoring higher order corrections. A four-parameter fit should produce the exponents but is numerically difficult and uncertain. We therefore fix Δ at its field theory value[8] of 0.475 instead and then do a three-parameter fit. The fit becomes linear if we take logs and expand the last term in Eq. (5.13) (see Fig. 10):

$$\log \langle S^2 \rangle_n = \log B + 2\nu \log n + Cn^{-\Delta} \tag{5.14}$$

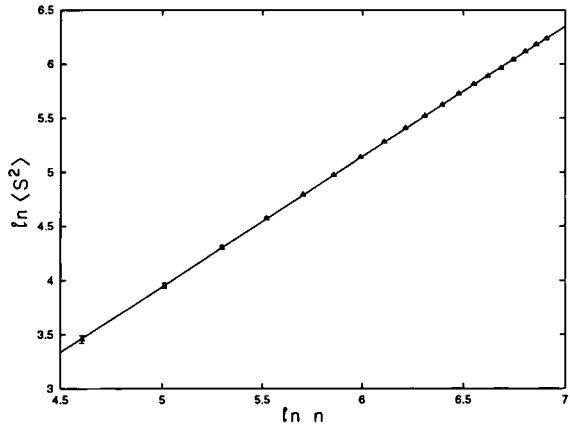

Fig. 10. Log–log plot of the mean-squared radius of gyration $\langle S^2 \rangle$ as a function of the length n of the ribbon.

A linear least squares fit gives

$$\nu = 0.591 \pm 0.004 \tag{5.15}$$

a value which, within the error bars, is close to previous estimates of ν for the self-avoiding walk in $d = 3$. Li *et al.*[26] found 0.5877 ± 0.0006 using the pivot algorithm for self-avoiding walks, and a series analysis by Guttmann gives 0.592 ± 0.002,[27] while Rapaport found 0.592 ± 0.004.[28] The field theory estimate is 0.588 ± 0.002.[8]

5.5. Entanglement Properties of the Ribbon

The entanglement complexity of the ribbon may be characterized by entanglement properties of the boundary curves, including linking, knotting, and writhing. The entanglement complexity of polygons and self-avoiding walks has been studied with reference to knotting, linking, and writhing both by numerical means[29–35] and analytic means.[30, 35–37, 2, 38] The polygons or walks were unconstrained in these studies, or confined to restricted spaces.[35, 39] In the ribbon model we may view the boundary curve of the ribbon as one polygon (nonorientable ribbon) or two polygons (orientable ribbon) naturally constrained to model the properties of double-stranded polymers. The entanglement complexity of these polygons may be studied by considering linking between them in an oriented ribbon, or the knotting if the ribbon is not oriented. Lastly, the writhe of these polygons is a natural "geometric" measure of complexity, as opposed to the topological measures such as linking and knotting.

The Link Probability of Boundary Components. If a ribbon is orientable, then double twists about its axis will link its boundary curves. If the midline of the ribbon is unknotted, then the links are all $(2,k)$-torus links and these may be characterized by computing their linking number. This is done as follows: Suppose that an orientable ribbon R has boundary curves C_1 and C_2. Orient these boundary curves in parallel, and consider their image projected onto a plane whose normal has irrational direction cosines. Since no vertex in either C_1 or C_2 (with integer coordinates) will project onto images of edges or vertices, all double points in the projection will be transverse and we may indicate overpasses and underpasses with due reference to the orientation as in Fig. 11. These are the signed crossings.

The sum over the signed crossings between the boundary curves is the *linking number* or Gaussian invariant of the link, indicated by $Lk(C_1, C_2)$. The curves C_1 and C_2 are *homologically* linked if and only if their linking number is nonzero.[40] This is an invariant property of the link, since it does not change under ambient isotopy or under interchanging C_1 and C_2. Reversing orientation on one boundary curve will change its sign. Ribbons with midlines which are nontrivial knots also admit homologically linked boundary curves, and this is also detected by computing the Gaussian invariant of the link, exactly as above. In these cases it is possible that topologically linked curves may not be homologically linked. We expect these cases to be rare for short ribbons, since the knotting probability is so low in that regime (we expect this since short polygons are known to have a very low know probability[33]).

The linking numbers of the boundary curves of the orientable ribbons were computed and collected as a function of the number of plaquettes n in the ribbon. These are plotted in Fig. 12; we plot the probability of homological linking (nonzero linking number) as a function of $1/\sqrt{n}$. The relationship turn out to be linear, and a least squares analysis gives slope -2.71 and intercept 1.00. In other words, the probability of linked boundary

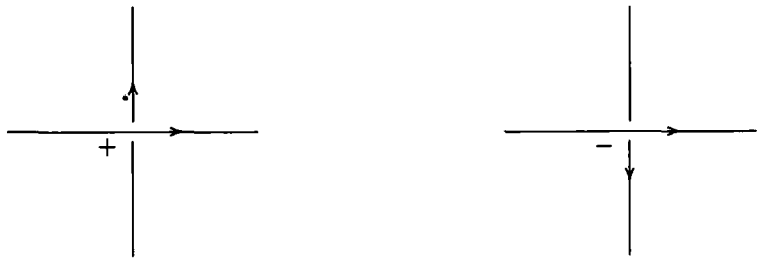

Fig. 11. Signed crossings determined by a right-hand rule.

curves increases to 1 as an inverse square root of the length of the ribbon. The probability that the boundary curves are not linked is inversely proportional to the square root of n. Nonrigorously, this observation may be explained by imagining homological linking to be the result of double twists in the ribbon. Since these can be left- or right-handed, an assumption of independence will give the square root law. The data in Fig. 12 suggest near independence of the twists. The probability of linking between the boundary components of the ribbon is much higher than the linking between polygons constrained inside a box,[35] and thus two polygons which are constrained to be the boundary curves of a ribbon are much more likely to be linked compared to polygons constrained by a confinging geometry.

The distribution of linking numbers with n is plotted in Fig. 13. If n is small, then a large proportion of ribbons have unlinked boundary components, but this fraction decreases rapidly with increasing n. The fraction of ribbons with boundaries which are linked with linking number equal to 1 or 2 increases rapidly with n, and soon overtakes the fraction of unlinked boundary curves. Asymptotically, these curves all tend to zero, as ribbons with higher linking number become feasible with increasing n.

Writhe of the Ribbon. The writhe of a curve is the mean of the summed signed crossings over all the oriented regular projections of the curve into the plane. In any oriented regular projection, double points are transverse (as in Fig. 11). Thus, to compute the writhe of a curve, an average must be taken over all the possible projections of the curve, summing the

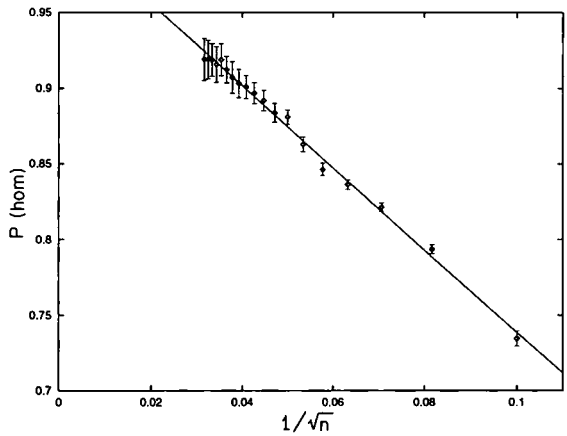

Fig. 12. The homological linking probability for the two boundaries of oriented ribbons as a function of $1/\sqrt{n}$, where n is the number of plaquettes in the ribbon.

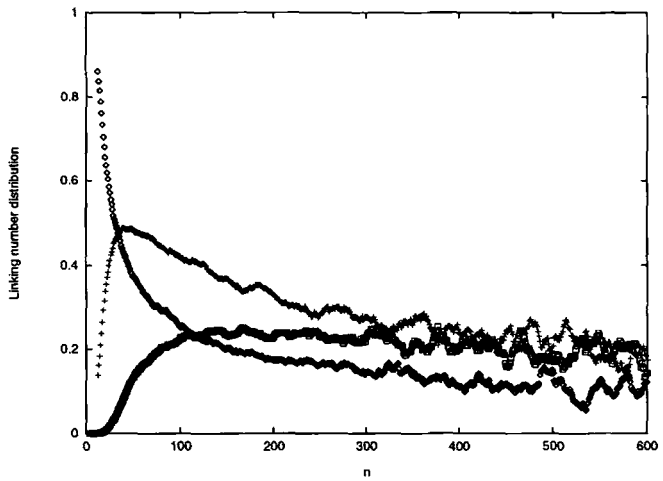

Fig. 13. Plot of distributions of occurrences of oriented ribbons as a function of their length n, normalized by the total number of occurrences, for three different linking numbers, $Lk = 0$ (diamonds), $Lk = 1$ (plusses), and $Lk = 2$ (squares).

signs on the crossings in each.[10] This procedure is greatly simplified when polygons in the cubic lattice are considered: A theorem of Lacher and Sumners[41] states that the writhe of a polygon in the cubic lattice is the average of the linking numbers of the polygon with four of its pushoffs (over small distances) into nonantipodal octants. Writhe is a geometric property of a curve which measures supercoiling. The mean of the absolute value of the writhe $\langle |Wr| \rangle$ is not zero, and this is the quality that we will study.

The mean absolute writhe of a polygon scales with the length n as

$$\langle |Wr| \rangle \sim n^{\zeta} \tag{5.16}$$

where it is known that $\zeta \geqslant 0.5$.[30] Numerically, ζ is close to 0.5. If we replace the polygon by the boundary components of the ribbon, then we expect similar behavior. In addition, we expect the mean absolute writhe to depend on the linking number of the boundary curves, and we analized our data in this respect. Figure 14 gives a log–log plot of $\langle |Wr| \rangle$ against n for linking numbers 0,1, and 2. Increasing linking number also increases writhe for any fixed n, but the curves seem to be asymptotic to the curve with linking number 0. The data of the curves corresponding to linking numbers 0 and 1 are well described by a linear fit, and we obtain $\zeta = 0.54 \pm 0.02$ for linking number 0 and $\zeta = 0.48 \pm 0.02$ for linking number 1 (95% confidence intervals). These values are close to the polygon value,[30] seemingly

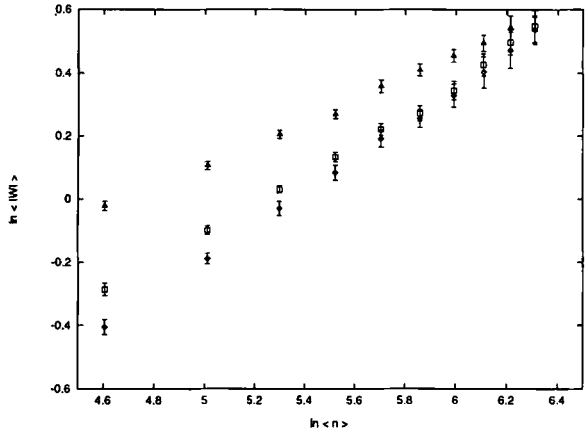

Fig. 14. Log–log plots of the man of the absolute value of the write of the boundary curves of oriented ribbons as a function of the length of the ribbon. The three curves correspond to the cases in which the boundary curves have linking number $Lk = 0$ (diamonds), $Lk = 1$ (squares), and $Lk = 2$ (triangles).

independent of linking number. The ribbon behaves essentially like a polygon, its writhe being determined by its polygon-like backbone.

Knot Probability for the Boundary of the Nonorientable Ribbon. A unoriented ribbon has one boundary curve which can be knotted. If the midline of the ribbon is unknotted, then the boundary curve may be a $(2, k)$-torus knot, and if the midline is a knot K, then the boundary will be a satellite knot of K. Unconstrained polygons, in constrast, may admit any knot type. The knot type of a polygon may be detected by computing the Alexander polynomial $\Delta(t)$ at $t = -1$. If $\Delta(-1) \neq 1$, then the polygon is a knot. There exist examples of knots with $\Delta(-1) = 1$ but the simplest example has ten crossings, and such knots are rare for short polygons.[33] We may therefore safely assume that the polygon is an unknot if $\Delta(-1) = 1$.

The probability that a polygon is an unknot goes to zero exponentially fast with increasing length[2, 38]:

$$P^0(n) = e^{-\alpha_0 n + o(n)} \tag{5.17}$$

for some positive constant α_o. This result is also true when the polygon is confined to a slab.[42] While we expect (5.17) to be the asymptotic behavior of $P^0(n)$, a different argument involving double twists in the ribbon and a coin tossing argument, similar to the argument which produced Fig. 12, indicate that $P^0(n) \sim 1 - B/\sqrt{n}$ for small values of n. This behavior will

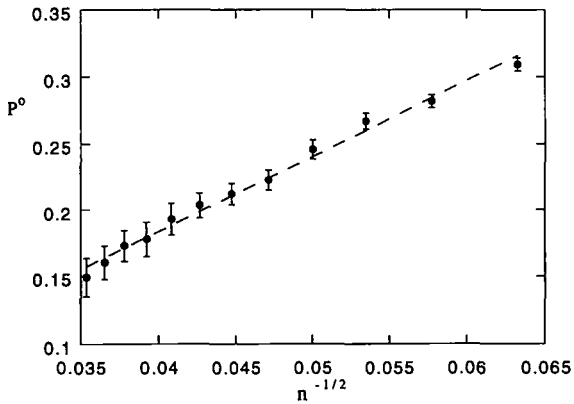

Fig. 15. Plot of $P^0(n)$ for the boundary curve of unoriented ribbons as a function of the length $1/\sqrt{n}$ of the curve. The line is a least square fit.

eventually be overtaken by the exponential behavior in (5.17). In our situation, we are at sufficiently small values of n to expect the square-root behavior, rather than the exponential behavior. This expectation is realized in Fig. 15. The straight line shown is a linear least squares fit; we found $B \sim 5.67$. This behavior will eventually break down completely as (5.17) becomes the dominant behavior. In the regime in Fig. 15 we expect to see

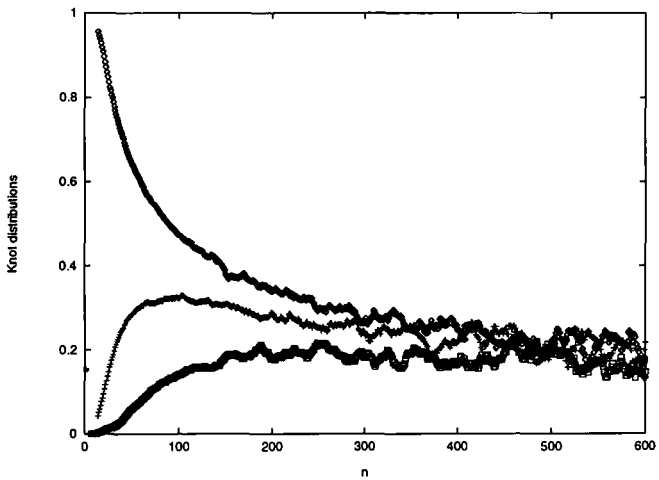

Fig. 16. Relative fractions of three different knot types in the boundary curves of unoriented ribbons as a function of their size n. The three sets of data correspond to the unknot (diamonds), trefoil (plusses), and knots of type 5_1 (squares).

mostly $(2, k)$-torus knots, and we plot the relative fractions of these against n in Fig. 16. The unknot peaks at small n and then rapidly decreases with increasing n, while nontrivial knots increase. The fraction of trefoils peaks at n roughly equal to 100, and after that it declines, while the fraction of knots of type 5_1 increases to peak around 250. These $(2, k)$-torus knots are the results of double twists in the ribbon (plus one single twist), which we assume to be independent in determining the square-root behavior visible in Fig. 15. The arguments which realize the exponential behavior in (5.17) are based upon the occurrence of satellites of nontrivial knots in the boundary of the ribbon, and in particular the satellites of compound knots. In the large-n limit these are the knots which will dominate, but it seems that our data are far from that regime.

6. CONCLUSIONS

Polymers (such as DNA and RNA) can exist in duplex forms in which one polymer chain twists around another chain, forming structures which are locally helical. Standard models for linear polymers, such as the self-avoiding walk, cannot describe the local degree of freedom associated with this twist. The interaction of the two strands leads to an additional entropy contribution. Ribbon models have been used[4] to describe this type of structure. In this paper we have considered a modification of such models in which the ribbon lies on a lattice and can be regarded as a sequence of plaquettes, with some conditions describing self-avoidance and ensuring that the ribbon is a manifold. The lattice model has several advantages. The self-avoidance inherent in a lattice ribbon implies that the ribbon cannot be indefinitely twisted, and this mimics the behavior of real molecules, determined by constraints such as fixed bond lengths and angles and inter monomer forces.

It is relatively easy to establish some results about the asymptotic behavior using combinatorial methods. For instance, one can prove that the growth constant exists (using concatenation arguments) and lies between 4 and 9.[7] In addition, one can use integer arithmetic in computer calculations, which results in efficient data structures such as hash-tables, linked lists, etc.

We have described a Monte Carlo algorithm which samples along a realization of a Markov chain defined on the set of closed ribbons. The algorithm consists of two types of moves, one of which is a collection of local moves (involving only a few contiguous plaquettes) and the other of which is a global move, reminiscent of the pivot algorithm for walks and polygons. If local moves only are allowed, the Markov chain is reducible, and the ergodic classes are the knot types of the center polygon of the

ribbon. This will allow future calculations on ribbons with fixed knot type (of the center polygon) which will be interesting both mathematically and as a model of double-stranded polymers with fixed topological constraints. If global moves are also allowed, the Markov chain becomes irreducible. This is the case for the numerical work reported in this paper. The sampling is uniform for ribbons with each fixed number of plaquettes, and is a modified exponential distribution [see (4.8) and Section 3] in the number of plaquettes. Global moves can change the knot type of the center polygon, the orientability of the ribbon, and properties such as the writhe. Local moves are efficient at changing twist and linking number, but make only small changes in writhe.

We have investigated the efficiency of the algorithm by estimating numerically the exponent characterizing the decay of the autocorrelations. Our value of 2.5 is close to the expected best value of $4\nu = 2.35...$, so the algorithm is efficient. The global moves are a key contributor to this efficiency, but local moves are also important for local properties.

We find a value of the metric exponent ν which is close to that of a self-avoiding polygon. Collapsing the ribbon onto its center polygon gives a polygon (on a decorated cubic lattice), so that one expects the exponents to be the same. We have estimated the growth constant, and its value is quite close to the lower bound of 4. We have also shown that the expected value of the absolute value of the writhe increases like n^{ζ} with ζ being about 1/2. For nonorientable closed ribbons we have computed the knot probability of the boundary, and find that this goes to unity exponentially rapidly as the length of the boundary increases.

In a separate paper we shall present a proof of a pattern theorem for ribbons. Several results follow immediately from his. We show there that the knot probability goes to unity exponentially rapidly, and also that the expectations of the absolute values of the linking number, twist, and writhe increase at least as rapidly as $\sqrt{n}$.

ACKNOWLEDGMENTS

The authors acknowledge financial support from NSERC (Canada). We have also benefitted from numerous discussions with Carla Tesi and De Witt Sumners.

REFERENCES

1. N. Madras and G. Slade, *The Self-Avoiding Walk* (Birkhäuser, Boston, 1993).
2. D. W. Summers and S. G. Whittington, *J. Phys. A* **21**:1689 (1988).
3. J. Mazur and F. L. McCrackin, *J. Chem. Phys.* **49**:648 (1968).
4. W. R. Bauer, F. H. C. Crick, and J. H. White, *Sci. Am.* **243**:118 (1980).

5. A. V. Vologodskii and N. R. Cozzarelli, *Annu. Rev. Biophys. Biomol. Struct.* **23**:609 (1994).
6. D. A. Rees, *Polysaccharide Conformation*, in *MTP International Review of Science, Organic Chemistry Series One*, Vol. 7, G. O. Aspinall, ed. (Butterworths, 1973) p. 251.
7. E. J. Janse van Rensburg, E. Orlandini, D. W. Sumners, M. C. Tesi, and S. G. Whittington, *Phys. Rev. E* **50**:R4279 (1994).
8. J. C. Le Guillou and J. Zinn-Justin, *Phys. Rev. B* **21**:3976 (1980), *J. Phys.* (Paris) **50**:1365 (1989).
9. J. H. White, *Am. J. Math.* **91**:693 (1969).
10. F. B. Fuller, *Proc. Natl Acad. Socc USA* **91**:513 (1971).
11. G. Calugareano, *Czech. Math. J.* **11**:588 (1961).
12. S. Y. Shaw and J. C. Wang, *Science* **260**:533 (1993).
13. N. Madras, A. Orlitsky, and L. A. Shepp, *J. Stat. Phys.* **58**:159 (1990).
14. N. Metropolis, A. W. Rosenbluth, M. N. Rosenbluth, A. H. Teller, and E. Teller, *J. Chem. Phys.* **21**:1087 (1953).
15. B. Berg and D. Foerster, *Phys. Lett.* **106B**:323 (1981).
16. C. Aragão de Carvalho, S. Caracciolo, and J. Frolich, *Nucl. Phys. B* **251**:209 (1983).
17. E. J. Janse van Rensburg and S. G. Whittington, *J. Phys. A* **24**:5553 (1991).
18. R. Brower, Private communication (1991).
19. N. Madras and A. D. Sokal, *J. Stat. Phys.* **50**:109 (1988).
20. A. Berretti and A. D. Sokal, *J. Stat. Phys.* **40**:483 (1985).
21. S. Caracciolo and A. D. Sokal, *J. Phys. A* **19**:L797 (1986).
22. A. D. Sokal and L. E. Thomas, *J. Stat. Phys.* **54**:797 (1989).
23. S. Caracciolo, A. Pelissetto, and A. D. Sokal, *J. Stat. Phys.* **63**:857 (1991).
24. S. Caracciolo, A. Pelissetto, and A. D. Sokal, *J. Phys. A* **23**:4589 (1990).
25. S. Caracciolo, A. Pelissetto, and A. D. Sokal, *J. Stat. Phys.* **60**:1 (1990).
26. B. Li, N. Madras, and A. Sokal, Critical exponents, hyperscaling and universal amplitude ratios for two- and three-dimensional self-avoiding walks, Preprint (1994).
27. A. J. Guttmann, *J. Phys. A* **20**:1839 (1987).
28. D. C. Rapaport, *J. Phys. A* **8**:1328 (1975).
29. A. V. Vologodskii, A. V. Lukashin, M. D. Frank-Kamenetskii, and V. V. Anshelevich, *Sov. Phys.-JETP* **39**:1059 (1974).
30. E. J. Janse van Rensburg, E. Orlandini, D. W. Sumners, M. C. Tesi, and S. G. Whittington, *J. Phys. A: Math. Gen* **26**:L981 (1993).
31. A. V. Vologodskii, A. V. Lukashin, and M. D. Frank-Kamenetskii, *Sov. Phys.-JETP* **40**:932 (1975).
32. J. P. J. Michels and F. W. Wiegel, *Proc. R. Soc. A* **403**:269 (1986).
33. E. J. Janse van Rensburg and S. G. Whittington, *J. Phys. A* **23**:3573 (1990).
34. K. Koniaris and M. Muthukumar, *J. Chem. Phys.* **95**:2873 (1991).
35. E. Orlandini, E. J. Janse van Rensburg, M. C. Tesi, and S. G. Whittington, *J. Phys. A* **27**:335 (1994).
36. W. F. Pohl, In *Lecture Notes in Mathematics*, Vol. 894, (1981), p. 113.
37. B. Duplantier, *Commun. Math. Phys.* **82**:41 (1981).
38. N. Pippenger, *Discrete Appl. Math.* **25**:273 (1989).
39. J. P. J. Michiels and F. W. Wiegel, *J. Phys. A* **22**:2393 (1989).
40. D. Rolfsen, *Knots and Links* (Publish or Perish, Wilmington, Delaware, 1976).
41. R. C. Lacher and D. W. Sumners, Data structures and algorithms for the computation of topological invariants of entanglements: Link, twist and writhe, in *Computer Simulations of Polymers*, R. J. Roe, ed. (Prentice-Hall, Englewood Cliffs, New Jersey, 1991), p. 365.
42. M. C. Tesi, E. J. Janse van Rensburg, E. Orlandini, and S. G. Whittington, *J. Phys. A* **27**:347 (1994).